Biogeosciences Discuss., 12, 19861–19900, 2015
www.biogeosciences-discuss.net/12/19861/2015/
doi:10.5194/bgd-12-19861-2015

Biogeosciences Discussions
Open Access
EGU

Heterotrophic bacterial production and metabolic balance during the VAHINE mesocosm experiment in the New Caledonia lagoon

F. Van Wambeke[1], U. Pfreundt[2], A. Barani[1], H. Berthelot[1], T. Moutin[1], M. Rodier[3,a], W. R. Hess[2], and S. Bonnet[1,3]

[1]Aix Marseille Université, CNRS/INSU, Université de Toulon, IRD, Mediterranean Institute of Oceanography (MIO) UM110, 13288, Marseille, France
[2]University of Freiburg, Faculty of Biology, Schaenzlestr. 1, 79104 Freiburg, Germany
[3]Mediterranean Institute of Oceanography (MIO) – IRD/CNRS/Aix-Marseille University IRD Nouméa, 101 Promenade R. Laroque, BPA5, 98848, Nouméa CEDEX, New Caledonia
[a]now at: IRD, Université de la Polynésie française – Institut Malardé – Ifremer, UMR 241 Ecosystèmes Insulaires Océaniens (EIO), IRD Tahiti, PB 529, 98713 Papeete, Tahiti, French Polynesia

Received: 24 November 2015 – Accepted: 27 November 2015 – Published: 11 December 2015

Correspondence to: F. Van Wambeke (france.van-wambeke@mio.osupytheas.fr)

Published by Copernicus Publications on behalf of the European Geosciences Union.

Abstract

N_2 fixation fuels ~ 50 % of new primary production in the oligotrophic South Pacific Ocean. The VAHINE mesocosm experiment designed to track the fate of diazotroph derived nitrogen (DDN) in the New Caledonia lagoon. Here, we examined the temporal dynamics of heterotrophic bacterial production during this experiment. Three replicate large-volume (~ 50 m^3) mesocosms were deployed and were intentionally fertilized with dissolved inorganic phosphorus (DIP) to stimulate N_2 fixation. We specifically examined relationships between N_2 fixation rates and primary production, determined bacterial growth efficiency and established carbon budgets of the system from the DIP fertilization to the end of the experiment (days 5–23). Heterotrophic bacterioplankton production (BP) and alkaline phosphatase activity (APA) were statistically higher during the second phase of the experiment (P2: days 15–23), when chlorophyll biomass started to increase compared to the first phase (P1: days 5–14). Among autotrophs, *Synechococcus* abundances increased during P2, possibly related to its capacity to assimilate leucine and to produce alkaline phosphatase. Bacterial growth efficiency based on the carbon budget was notably higher than generally cited for oligotrophic environments (27–43 %), possibly due to a high representation of proteorhodopsin-containing organisms within the picoplanctonic community. The carbon budget showed that the main fate of gross primary production (particulate + dissolved) was respiration (67 %), and export through sedimentation (17 %). BP was highly correlated with particulate primary production and chlorophyll biomass during both phases of the experiment but slightly correlated, and only during P2 phase, with N_2 fixation rates. Our results suggest that most of the DDN reached the heterotrophic bacterial community through indirect processes, like mortality, lysis and grazing.

BGD
12, 19861–19900, 2015

1 Introduction

In the South West Pacific ocean, the natural occurrence of abundant and diverse plankton taxa capable of dinitrogen (N_2) fixation (N_2-fixing or diazotrophic organisms) (e.g., Moisander et al., 2010) can fuel ~ 50 % of new primary production. (Garcia et al., 2007; Bonnet et al., 2015c). However, little is known about the fate of the diazotroph-derived nitrogen (DDN) in this environment (Bonnet et al., 2015b). In particular, the role played by the microbial food web, and among them the heterotrophic bacteria in the transformation of DDN is largely unknown. In the central gyre of the South Pacific, where N_2 fixation is lower than in the South West Pacific, nitrogen is the first element limiting growth of both phytoplankton and heterotrophic bacterioplankton as observed in short-term nutrient enrichment experiments (Bonnet et al., 2008; Van Wambeke et al., 2008a) or incubations with ^{15}N-leucine or ^{15}N-NH_4^+, which significantly enhanced bicarbonate uptake (Halm et al., 2012). Such competition for nitrogen influences dissolved organic carbon accumulation in the surface layers and export. In the South West Pacific, however, the phytoplankton – heterotrophic bacterial coupling has mainly been investigated in the New Caledonia Lagoon. In this system, phytoplankton and bacterial production show seasonal patterns, with maxima in December–January and annual bacterial production representing 21 to 34 % of particulate primary production (Torreton et al., 2010), In the oligotrophic stations of the lagoon, based on a bacterial growth efficiency of 10 % or less, dissolved phytoplankton release was shown to be not sufficient to sustain bacterial carbon demand (Rochelle-Newall et al., 2008). N-limitation of primary production is expected based on year-round dissolved inorganic nitrogen (DIN) to dissolved inorganic phosphorus (DIP) ratios and silicates to DIN ratios, respectively lower and higher than Redfield ratios (Torréton et al., 2010). However, N_2 fixation is a recurrent feature in the lagoon (Garcia et al., 2007; Biegala and Raimbault, 2008), and no information is available on the potential role played by this process on the functioning of the microbial food web and how it could influence the factors limiting heterotrophic bacterial production. As blooms of diazotrophs are transient events, the

BGD
12, 19861–19900, 2015

production of varying sources and quality of organic matter is expected, which may influence biogeochemical fluxes, in particular heterotrophic bacterial production.

Through the VAHINE program (http://mio.pytheas.univ-amu.fr/?VAHINE-Project; Bonnet et al., 2015b), we experimentally investigated the fate of DDN in the planktonic food web and its potential impact on particle export. For this, we studied the development and the fate of a diazotroph bloom enhanced by intentional fertilization with DIP in large-volume ($\sim 50\,m^3$) mesocosms deployed in the New Caledonian lagoon, DIP being considered to control the nitrogen input by dinitrigen fixation in the SW Pacific upper surface waters (Moutin et al., 2005, 2008). The VAHINE experiment provided a unique opportunity to study such phytoplankton-heterotrophic bacteria interactions by simultaneously using biogeochemical techniques assessing stocks and fluxes in the same body of water for a period of 3 weeks. In particular, our objectives were, (i) to explore factors controlling heterotrophic bacterial growth, (ii) to examine the links between heterotrophic bacterial production and the activity of N_2-fixing organisms and primary producers and (iii) to study the fate of carbon inside mesocosms and the balance of autotrophy vs. heterotrophy. The factors controlling heterotrophic bacterioplankton were studied using short-term nutrient enrichment experiments and measurements of alkaline phosphatase activity. In oligotrophic systems, assimilation of organic nitrogen-containing molecules can also confer advantage for growth to some cyanobacteria (Zubkov et al., 2004; Mary et al., 2008a). Thus we quantified fluxes of leucine incorporation on a single cell basis, using flow sorting by cytometry (Talarmin et al., 2011).

2 Material and methods

2.1 Mesocosm description and sampling strategy

Three large mesocosms ($\sim 50\,m^3$) were deployed as open tubes with unfiltered, nutrient-poor, waters of the Nouméa lagoon close to the Boulari passage

BGD
12, 19861–19900, 2015

(22°29.073′ S–166°26.205′ E) located 28 km of the coast from 13 January to 4 February 2013 (Fig. 1). After 2 days for stabilizing mixing and verticality of mesocosms, they were closed at their bottom, which constituted the starting day of the experiment, and a sediment trap was screwed at the basis of the bottom cone of each mesocosm and changed every morning by SCUBA divers. The mesocosms design is based on Guieu et al. (2010) and the choice of the site in the lagoon, deployment and sampling strategy are described in details in Bonnet et al. (2015b). The three triplicate mesocosms were supplemented with 0.8 µM KH_2PO_4 between day 4 and day 5 of the experiment to alleviate potential P limitation and induce a bloom of naturally present communities of N_2 fixing organisms. All samples for the parameters described below were collected every morning for 23 days using a clean Teflon pumping system from three selected depths (1, 6, 12 m) in each mesocosm (M1, M2 and M3) and in surrounding waters (i.e. outside the mesocosms, hereafter called Nouméa lagoon waters). Seawater from each mesocosm was first filled in a polypropylene 50 L tank for stocks measurements, 4.5 L polycarbonate bottles for rates measurements and 10 L carboys for diversity. All carboys were immediately transferred onto the R/V *Alis* anchored close to the mesocosms to serve as a lab platform to ensure a quick processing of the samples. Subsampling procedure and analysis for inorganic nutrients, chlorophyll *a* (Chl) and their associated phaeopigments, DIP turnover time and N_2 fixation rates are detailed in a companion paper (Berthelot et al., 2015). Primary production (PP) is determined from short term (∼ 4 h) incubations around noon using ^{14}C labeling technique (see details in Berthelot et al., 2015) and a model of photosynthesis is then applied which restitute daily fluxes (Moutin et al., 1999).

2.2 Heterotrophic bacterioplankton abundances

Flow cytometry analyses were carried out at the PRECYM flow cytometry platform (https://precym.mio.univ-amu.fr/). Samples were analyzed using a FACSCalibur (BD Biosciences, San Jose, CA). For heterotrophic bacterial abundance (BA), 1.8 mL of seawater was fixed with formaldehyde (2 % final concentration, 15 min incubation at

BGD
12, 19861–19900, 2015

RT), frozen and stored in liquid N_2 until analysis in the laboratory. After thawing at room temperature, 0.3 mL of each sample was incubated with SYBR Green II (Molecular Probes, final conc. 0.05 % [v/v]) for 15 min at room temperature in the dark) to stain nucleic acids (Marie et al., 1997). Cells were characterized by 2 main optical signals collected from the 488 nm laser: side scatter (SSC, related to cell structure) and green fluorescence ($530/40_{488\,nm}$), related to nucleic acids staining. For the calculation of heterotrophic prokaryotes abundances, phytoplankton, in particular *Prochlorococcus* and *Synechococcus*, was gated out thanks to its red autofluorescence induced by the chlorophyll (Sieracki et al., 1995). We discriminated HNA (high nucleic acid) and LNA (low nucleic acid) cells and heterotrophic bacterial abundance (HBA) was calculated as the sum of both categories. TruCount beads (BD Biosciences) and 2 µm beads (Fluoresbrite YG, Polyscience) were added to the samples just before analysis. To determine the volume analyzed by the flow cytometer, the flow rate was estimated by weighing three tubes of samples before and after a 3 min run. The cell abundance was determined by dividing the number of cells by the volume analyzed determined both by the TruCount beads and flow rate. All data were collected in log scale and stored in list-mode using the CellQuest software (BD Biosciences). Data analysis was performed using the SUMMIT v4.3 software (Dako).

2.3 Heterotrophic bacterial production

Heterotrophic bacterial production (BP) was estimated daily using the ^{3}H-leucine incorporation technique (Kirchman, 1993), adapted from the centrifuge method (Smith and Azam, 1992). For each sample, triplicate aliquots (1.5 mL) and one trichloroacetic acid (TCA) killed control were incubated with a mix of 6 nM hot leucine (L-[^{3}H] leucine, Perkin Elmer® specific activity ranging 106 Ci mmol^{-1}) and 14 nM cold leucine, at in situ surface temperature (on-deck incubators equipped with 50 % light intensity screen and cooled with circulating surface seawater), for 1 h. Linearity of leucine incorporation was checked regularly by time series experiments. The live incubations were terminated with 5 % TCA (final concentration). After three runs of centrifugation/aspiration

BGD
12, 19861–19900, 2015

of the supernatant (once with the fixed sea water sample, once with a 5 % TCA rinse, once with an 80 % ethanol rinse), the pellet was resuspended in Packard Ultima Gold MW Scintillation liquid®. Radioactivity was counted using a Liquid Scintillation Analyzer Packard® 1600TR and the ^{3}H counting efficiency was corrected for quenching. Concentration kinetic experiments showed that isotopic dilution factor ranged 1 to 1.56 and thus BP rates were calculated from leucine incorporation rates using conversion factor adjusted from 1.5 to 2.4 kg C mol^{-1} leucine. Daily rates were calculated assuming they are 24 times the hourly rate.

2.4 Specific leucine assimilation assessment using cell sorting

On four occasions (day 15, M1, 6 m; day 19, M1, 6 m; day 21, lagoon waters, 1 m; day 23, M3, 1 m), additional seawater samples were incubated with ^{3}H leucine for further cell sorting of phytoplankton and heterotrophic bacteria: five polypropylene (Nunc) tubes (3 live samples, 2 killed controls) were filled with 4.5 mL of seawater and incubated with pure ^{3}H leucine (10 nM final conc.) for 1 h in the on-deck incubator as for bulk samples (Sect. 2.3). Incubations were stopped by addition of 0.5 mL of 20 %, 0.2 µm-filtered formalin, stored in the fridge for 15 min, and then stored in liquid N_2 until sorting. Two additional non-incubated tubes (but fixed and stored in the same conditions) were used for total counts. Sorting of the radiolabeled samples were performed with on a BD Influx™ Mariner (BD Biosciences, San Jose, CA) high speed cell sorter equipped with three laser lines: 488 nm (Sapphire, Coherent), 561 nm (Jive, Cobolt) and 355 nm (Xcyte, JDSU). All data were collected in log scale, stored in list mode files and analyzed in real time for sorting using the BD FACSortware software (BD Biosciences), or analyzed a posteriori using FlowJo v7.6.5 software (Tree Star). A solution of 0.5x PBS, 0.2 µm filtered, was used as sheath fluid. For heterotrophic prokaryote analyses and sorting, (using a drop purity sort mode), cells were stained with SYBR Green II as described above in Sect. 2.2. Cells were characterized by two main optical signals collected from the 488 nm laser: side scatter (SSC) and green fluorescence ($530/40_{488\,nm}$), related to nucleic acid staining. Based on these criteria, low

BGD
12, 19861–19900, 2015

nucleic acid (LNA), high nucleic acid (HNA), and HNA with high SSC (Hi-HNA) groups were determined (Fig. 2) and sorted into different tubes. Like for determination of LNA and HNA abundances (Sect. 2.2), phototrophic cells were excluded thanks to their red fluorescence. To analyze and sort the photosynthetic phytoplankton cells, the three laser lines were used. Red fluorescence ($630LP_{488\,nm}$) related to chlorophyll *a* content, was used as trigger signal. Phytoplankton cells were characterised by three other optical signals: forward scatter (FSC) related to cell size, side scatter (SSC), and the orange fluorescence ($580/30_{488\,nm}$) related to phycoerythrin. In addition, the chlorophyll *a* red fluorescence was collected from the 355 and 561 nm excitation ($630LP_{355\,nm}$ and $630LP_{561\,nm}$). The cytogram red fluorescence (induced by the 561 nm laser) vs. orange fluorescence induced by the 488 nm laser evidenced two different subgroups of *Synechococcus* (one with Low and one with a High Orange fluorescence intensity, referred to as LO-SYN and HO-SYN, respectively, Fig. 2). Thus, four populations < 2 µm were optically resolved and sorted simultaneously, directly into separate 2 mL Eppendorf centrifuge tubes, using the drop purity sort mode: *Prochlorococcus* (PRO), LO-SYN and HO-SYN, and pico-eukaryotes (PE).

Variable numbers of cells were sorted per sample depending on experiment and cell type, to achieve sufficient signal and a good compromise with the volume available. The phytoplankton collected cells ranged from 50 000–279 000 for the LO-SYN and HO-SYN groups, 16 000–41 000 for the PE, to 1600–10 000 for the PRO group. From the 1 mL SYBR Green II stained aliquot, the three heterotrophic prokaryote groups were simultaneously collected into separate 2 mL centrifuge plastic tubes, collecting a range of 100 000–250 000 cells for LNA and HNA groups, and 15 000–53 000 cells for Hi HNA group. After sorting, 1.5 mL of 5 % TCA was added into each tube and processed as for BP measurements. Bulk activities were realized in triplicate by subsampling directly 1.0 to 1.5 mL of samples from the 5 mL tubes. In these tubes, 55 % TCA was added to give a final 5 % TCA concentration and the three series of centrifugations were run as for the BP measurements. Formalin-killed samples were also sorted in order to estimate blank values for each group. Dpm in the killed control of a given group were

BGD
12, 19861–19900, 2015

subtracted from dpm in the corresponding incubated sample. Blank values were independent of the number of sorted cells (on average 27 ± 9 dpm). We checked that a linear increase of the dpm signal occurred with the number of sorted cells. The coefficient of variation between triplicate sorts ranged 1–5 % when dpm signal were > 1000 dpm, but these values increased up to 30 % when the dpm signal were < 100 dpm due to methodological limitations (limited volume available or lower activities). For this reason we considered below detection limits all sorts where dpm values were less than twice the corresponding blank value. The radioactivity per cell was calculated and expressed in C units (10^{-21} mol leu cell^{-1} h^{-1}). It was multiplied by the abundance of cells mL^{-1} within in sorted region to obtain the volumetric incorporation rate of each group, and the relative population activity was calculated as the population fraction of the bulk (i.e. total community) activity. The effect of a long storage of the samples before cell sorting was checked by counting abundance of cells mL^{-1} directly on the Influx. For this, we used the additional non labeled tubes, ran using similar procedure (sample preparation with control beads, and flow rate determination) as described in Sect. 2.2., except that we counted also Hi-HNA cells and the two categories of *Synechococcus*.

2.5 Nutrient addition experiments

The availability of phosphorus (P), nitrogen (N) and organic carbon (C) for heterotrophic bacteria was investigated by measuring changes in bacterial production following additions of DIP (0.25 µM P), NO_3^- and NH_4^+ (1 µM each) or glucose (10 µM C) (final concentrations). Two bioassays were realised, one right before (day 4) and one two weeks after (day 20) the DIP fertilization in M1 (samples from 1 m depth). Eight combinations were tested (P, N, C, PN, PC, NC and PNC) including the non-enriched control T. Each bioassay condition was tested in triplicate in 60 mL polycarbonate bottles incubated for 48 h under in situ-simulated conditions in the on-deck incubator (described in Sect. 2.3). After incubation, each bottle was sub-sampled in order to measure BP using the leucine technique described in Sect. 2.3.

BGD
12, 19861–19900, 2015

2.6 Alkaline phosphatase activity

Total alkaline phosphatase activity (APA) was measured at the three depths in M1, M2 and M3 and in Nouméa lagoon waters using the analog substrate methylumbelliferone phosphate (MUF-P, 1 µM final concentration) (Hoppe, 1983). The linear increase in fluorescence of seawater with added MUF was measured over the incubation time (up to 8 h), in the dark with a TKO 100 Hoefer DNA fluorometer (single-wavelength with excitation/emission fixed at 365/460 nm but suitable for MUF). Concentration kinetics using a range from 25 to 2500 nM MUF-P were run on some occasions to check that the 1 µM concentration used for routine measurements was sufficient to saturate enzyme activity. Blanks were run by adding the MUF-P to filtered boiled seawater and were shown to be insignificant. Calibration curves were made with MUF standards.

2.7 Statistical analyses

Non parametric Mann–Whitney and Kruskal–Wallis tests were used to compare differences of each parameter studied between mesocosms, periods of time, or effect of various amendments on BP in the nutrient addition experiments. Model I linear regressions and Pearson correlation coefficient were used to study Log–log relationships between BP and Chl or PP; and evolution of DOC and POC with time.

3 Results

Very little vertical stratification was observed in the mesocosms for bacterial production or alkaline phosphatase activity (APA) (see examplary data for M1 in Fig. 3) as for most of the parameters (Bonnet et al., 2015b; Turk-Kubo et al., 2015; Berthelot et al., 2015). For all description of biogeochemical stocks and fluxes, we thus used the average of the three depths to plot the temporal evolution within each mesocosm.

BGD
12, 19861–19900, 2015

3.1 Chlorophyll stocks and net primary production

Based on the Chl and PP dynamics, two periods P1 (days 5–14) and P2 (days 15–23) were identified after DIP fertilization, which were also identified by Berthelot et al. (2015) based on biogeochemical characteristics and by Turk-Kubo et al. (2015) based on changes in abundances of targeted diazotrophs. Diatom heterocyst-forming symbionts associated with diatoms were abundant during P1 while a bloom of the unicellular N_2-fixing cyanobacteria from Group C (UCYN-C) occurred P2 (Leblanc et al., 2015; Turk-Kubo et al., 2015). Chl stocks significantly increased during P2 compared to P1 in the three mesocosms (statistics are presented in Table 1). Chl concentrations during P2 in all three mesocosms were significantly higher than those in the Nouméa lagoon for the same period. PP showed the same trend as for Chl, being higher during P2 in all three mesocosms (Fig. 4, Table 1). However, the PP rates and Chl concentrations reached during P2 were not identical between the three mesocosms: M3 exhibited higher Chl concentrations during P2 ($0.71 \pm 0.30\,\mu g\,L^{-1}$) than M2 ($0.49 \pm 0.18\,\mu g\,L^{-1}$) and M1 ($0.42 \pm 0.14\,\mu g\,L^{-1}$, $p < 0.001$). This was equally true for PP rates ($2.45 \pm 0.76\,\mu mol\,C\,L^{-1}\,d^{-1}$ in M3 compared to $1.47 \pm 0.35\,\mu mol\,C\,L^{-1}\,d^{-1}$ in M2 and $1.09 \pm 0.22\,\mu mol\,C\,L^{-1}\,d^{-1}$ in M1, $p < 0.001$). Significant increases of Chl and PP were also observed in lagoon waters (reaching in P2 $0.30 \pm 0.07\,\mu g\,Chl\,L^{-1}$ and $1.36 \pm 0.37\,\mu mol\,C\,L^{-1}\,d^{-1}$, respectively, Table 1).

3.2 Heterotrophic bacterioplankton abundance and production

Abundances of heterotrophic bacterioplankton (HBA) varied 10 fold, from 1.7 (day 9, M1, 1 m) to 12.8×10^5 cells mL^{-1} (M2, day 11, 6 m). However peaks of HBA were sporadic and average HBA did not increase statistically between phase P1 and P2 in M1 and M2 and increased slightly ($p < 0.05$) from (4.1 ± 0.7) to $(5.0 \pm 1.4) \times 10^5$ cells mL^{-1} in M3 (Table 1, Fig. 4). Evolution of BP in the mesocosms was close to that in lagoon waters during P1, except for a peak only detected on day 4 (the morning before DIP fertilization) in M1 and M3, and at day 5 in M2. These peaks were not related to any HBA,

BGD
12, 19861–19900, 2015

Chl or PP increase but were related to a steep increase in *Rhodobacteraceae* 16S ribosomal RNA genes (Pfreundt et al., 2015b). Just like PP, BP significantly increased during P2 in all three mesocosms with higher values in M3 compared to M1 and M2 during P2 (Kruskal–Wallis test, $p < 0.05$). This BP increase was also observed in lagoon waters but with lower amplitude (Table 1). In the three mesocosms, the log–log relationship between BP and PP was significant only during P2 ($r = 0.54$, $p < 0.001$), whereas that between BP and Chl was significant during P1 and P2 ($r = 0.4$, $p < 0.001$ and $r = 0.72$, $p < 0.001$, respectively, Fig. 5). In lagoon waters, the BP/PP ratio slightly increased (but significantly) between P1 and P2 (0.33 to 0.39, $p < 0.05$, Table 1). The BP/PP ratio significantly increased during P2 in M1 (0.48 to 0.65, $p < 0.001$), significantly decreased in M3 (0.50 to 0.35, $p < 0.05$) and remained stable in M2 (Table 1). Such differences probably depended on varying maximal values of PP in different mesocosms and the exact days when PP or BP started to increase. Thus we examined the trend of BP/PP ratio with PP, keeping in mind the risk of autocorrelation. BP/PP ratio decreased when PP increased, with higher intensities in the mesocoms compared to lagoon waters, and consistent for P1 or P2 (Table 2). The log–log relationship between N_2 fixation rates ($nM\,d^{-1}$) and BP (mg C $m^{-3}\,d^{-1}$) was insignificant during P1 and significant during P2 ($\log BP = 0.13 \times \log(N_2 \text{ fix rates}) + 0.73$, $r = 0.21$, $p = 0.04$, data not shown).

3.3 Alkaline phosphatase activity

APA was homogeneous between the three depths sampled from the mesocosms (example for M1 on Fig. 3), but this was not the case in the Nouméa lagoon, where activity was often higher at 1 m depth compared to the two other depths (data not shown). A slight but very reproducible decrease of APA occured on days 5 and 6 in all three mesocosms where DIP fertilization took place, and in lagoon waters only on day 5 (Fig. 4). DIP was consumed more rapidly in M1, mirrored by higher APA and lower TDIP between day 9 and 18 in this mesocosm (Fig. 4). APA then increased very rapidly in M1 and M2 after day 17, but only after day 21 in M3. Such delays were in agree-

BGD
12, 19861–19900, 2015

ment with the evolution of DIP, which was less rapidly consumed in M3 compared to M1 and M2 (Berthelot et al., 2015). Consequently, although mean APA increased significantly in all three mesocosms between P1 and P2 (Table 1), it was lower in M3 compared to M1 and M2 during P2 (3.1 vs. 7.5–7.9 nmol MUF-P hydrolyzed $L^{-1}\,h^{-1}$, respectively, $p < 0.01$). Finally, APA also increased significantly between P1 and P2 in the lagoon waters, albeit to a lower extent as in the mesocosms (from 3 to 5 nmol MUF-P hydrolyzed $L^{-1}\,h^{-1}$, Table 1). Noteworthy, APA in the lagoon waters exhibited the strongest increase between day 10 and 11 and stayed at this higher level until day 23, thus exhibiting different dynamics than in the mesocosms.

3.4 Enrichment experiments

In the two 48 h nutrient enrichment experiments performed on day 4 and on day 20, BP increased 3-fold after nitrogen addition ($NH_4^+ + NO_3^-$) compared to the unamended controls. This significant increase was observed irrespectively of whether these N sources were added alone or in combination with DIP or glucose (N, NP, NG, NPG treatments, Fig. 6, $p < 0.03$). Only PG and G addition on day 4 led to significant BP increase without N addition ($p < 0.05$) however, to a much lower extent than with all N combinations (factor 1.5 and 1.1, respectively). On day 20, only N amendments led to significant BP increases after 48 h incubations, compared to the unamended control (Fig. 6, $p < 0.03$).

3.5 Cell-specific leucine incorporation rates

Among the different groups sorted by flow cytometry, significant cell-specific leucine incorporation rates into macromolecules were obtained for heterotrophic bacterioplankton. LNA, HNA and hi-HNA cells had specific activities ranging from 4.6 to 86×10^{-21} mol cell$^{-1}\,h^{-1}$. Overall, cell specific leucine incorporation rates for LNA cells were lower than or equal to rates for HNA cells, and rates for Hi-HNA cells were 1.2–4.8 times greater than rates for HNA cells (Table 3). All cell-specific rates increased when bulk activities increased. Among autotrophic groups, significant leucine incorpo-

BGD
12, 19861–19900, 2015

ration was detected for *Prochlorococcus* cells (PRO) only on day 21 and day 23, due to the low volume available for sorting and a significant decrease of PRO abundances in the samples to be sorted, when compared to the abundances determined on samples analysed only three months after the experiment. We checked on fresh Mediterranean samples that *Prochlorococcus* cells were clearly detectable with the flow cytometer setting chosen, and could discard any instrument problem. We assumed that the PRO cells lower detection was due to the long storage period of ^{3}H-leucine labelled samples until cell sorting (two years at −80 °C) that could induce a loss of fluorescence or cell damages. We obtained a maximum of 1200 PRO cells sorted. Thus, even when the signal was significant, it was associated with a high error (40 % on day 21, Table 3). On the opposite, *Synechococcus* cells (SYN) were well detected and their total abundance matched with the total counts determined on samples analysed three months after the experiment. Additional 651 and 355 nm laser excitations allowed us to distinguish two different sub-groups, not clearly distinguishable using only 488 nm laser excitation, separated mainly on the criterion of orange fluorescence (LO-SYN and HO-SYN) (Fig. 2), suggesting different relative amounts of accessory pigments (Neveux et al., 2010). Leucine incorporation was detected in both SYN groups for all samples analysed. For a given sampling date, cell specific rates of both groups were almost equal, and increased on day 21 and 23 compared to days 15 and 19. They were lower than LNA cell-specific rates (from ∼ 20 % of the LNA rates at day 15 to ∼ 70 % at day 21). Cell-specific rates of LO-SYN and HO-SYN diverged only on day 23 (Table 3). At this date, cell specific rates for LO-SYN were twice as high as for LNA cells, reaching 131×10^{-21} mol cell^{-1} h^{-1}. Overall, the contribution of the two *Synechococcus* groups to the bulk activity was very low: it ranged 0.2 to 0.7 % for LO-SYN or HO-SYN (i.e. the contribution reached a max of 1.5 % for both SYN groups together), and 0.01–0.02 % for PRO (when detected), respectively. Contribution of LNA cells to the bulk activity was 4–12 %. Thus, the most important contribution to the bulk leucine activity was due to HNA and Hi-HNA cells.

BGD
12, 19861–19900, 2015

4 Discussion

4.1 N limitation and coupling between BP and N_2 fixation

BP was significantly enhanced on a short-term scale (1–2 days) by $NO_3^- + NH_4^+$ but not DIP or glucose amendments, indicating that BP was directly N-limited, and/or indirectly after stimulation of N-limited phytoplankton (Fig. 5). In the New Caledonia lagoon, N-limitation has previously been suggested based on a one-year survey of nutrient ratios (Torréton et al., 2010). N-limitation is a recurrent feature observed in the ultra-oligotrophic South Eastern Pacific Gyre (Van Wambeke et al., 2008a; Halm et al., 2012), as assessed from short-term (1–3 days) enrichment experiments or incubations. As N_2 fixation is assumed to be the only process providing a source of new nitrogen to the mesocosms in this experiment, we examined the potential links between N_2 fixation rates and BP. First, marine heterotrophic diazotrophs were detected at low abundances during the mesocosms experiment: γ-24774A11 with ca 10^2–10^3 *nifH* gene copies L^{-1} (Turk-Kubo et al., 2015), and 16S tags corresponding to heterotrophic diazotrophs like *Bradyrhizobium* or *Mesorhizobium* were scarce (Pfreundt et al., 2015b). Therefore, N_2 fixation directly performed by heterotrophic bacteria probably accounted for a minor fraction of bulk N_2 fixation during the mesocosm experiment. Second, as the log–log relationship between N_2 fixation rates and bacterial production was not significant during P1, and only slightly significant during P2 (r = 0.21, p = 0.04), the excretion of DON and NH_4^+ by diazotrophs likely did not much supply much nitrogen for heterotrophic prokaryotes directly, particularly during P1 when the main organisms responsible for diazotrophy were diatom-symbiotic (Turk-Kubo et al., 2015). Assuming a C/N molar ratio of around 6.8 for heterotrophic prokaryotic biomass (Fukuda et al., 1998), N_2 fixation might have provided 17 to 30 % of the nitrogen demand of heterotrophic prokaryotes, depending on the phase and the mesocosm considered (Table 1). This proportion increases to 30–37 % if we consider a C/N ratio of 8.2, which seems more appropriate in the Pacific Ocean (Fukuda et al., 1998). Thus, N_2 fixation contributed to but was not sufficient to sustain 100 % of the N requirements of heterotrophic bacteria during

BGD
12, 19861–19900, 2015

this study. Other potential sources were initial DON stocks, concentrations of which decreased slightly at the end of the experiment (Berthelot et al., 2015) and detritus. Indeed, there was a decay of larger phytoplankton cells after the closure of the mesocosms as discussed by Knapp et al. (2015) and Leblanc et al. (2015) following DIP availability (TDIP) as well as PP decreases (Berthelot et al., 2015) and *Synechococcus* 16S tags dropped substantially between day 2 and 4 (Pfreundt et al., 2015b). Such detritus probably also contributed to sustain BP. NanoSIMS analyses were performed during a parallel experiment done at the height of a bloom of diazotrophic *Cyanothece*-like cyanobacteria (UCYN-C) on days 17–20 in M2 (Bonnet et al., 2015a). After 24 h of $^{15}N_2$-incubations, these authors reported significant ^{15}N-enrichment in picoplanktonic cells (0.2–2 µm fraction). This confirmed a rapid (one day) transfer of DDN (also ^{15}N-enriched) to picophytoplankton, and potentially heterotrophic bacteria. However, such transfer likely occurred indirectly through DON after mortality and grazing processes, as shown by model simulations run during the VAHINE project (Gimenez et al., 2015).

4.2 Cyanobacterial assimilation of leucine

BP was used in this study as a strict proxy of heterotrophic bacterial production. As we incubated ^{3}H leucine under light conditions, photoheterotrophic activity and the possibility that some photosynthetic cyanobacteria incorporate leucine could biases BP estimates. Whether light stimulation of bacterial production can be explained by direct (assimilation or organic molecules by autotrophs), or indirect effects (stimulation of BP through release of organic molecules or photo-labilization of organic matter), or both, is difficult to determine (Béjà and Suzuki, 2008). Assimilation of methionine, leucine, and ATP was shown to be enhanced under light-incubation conditions in the North and South Atlantic Oceans and these increases are generally attributed to stimulation of *Prochlorococcus* and SAR11 (Evans et al., 2015), but the spectrum of organic molecules tested is low. In the New Caledonia lagoon, incubation of samples under different light regimes influences estimates of BP determined by the thymidine technique (Rochelle-Newall et al., 2008), but so far there is no information available on

BGD
12, 19861–19900, 2015

the light effect on leucine uptake around New Caledonia. The capacity of both marine *Prochlorococcus* and *Synechococcus* to assimilate some organic molecules is evident from culture-studies, as well as flow cytometry cell sorting and gene studies (Béjà and Suzuki, 2008). Assimilation of leucine by cyanobacteria can also occur in the dark (Talarmin et al., 2011), but light clearly favours assimilation of leucine by cyanobacteria (Mary et al., 2008b). The polypropylene tubes used in this study to incubate BP attenuated the light intensity by 40 % without spectral distortion in the visible range (Richardson and Porter, 2005). Under such conditions which were intermediary between simulated in situ light conditions and dark conditions, significant incorporation of leucine into macromolecules was seen by flow cytometry sorting of *Synechococcus* cells. We could not unambiguously verify leucine incorporation into *Prochlorococcus* cells due to technical reasons (low volumes and long storage limitations). To conclude, although the relative contribution of cyanobacteria (PRO + SYN) to the bulk (community) leucine assimilation into proteins was less than 2 %, and could not be responsible of a bias in BP estimates, we estimate significant potential for leucine to be assimilated by cyanobacteria. Note that we used a 10 nM leucine concentration for cell sorting, but in situ natural concentrations could be much lower. More studies are needed, investigating the potential use of other organic molecules in lower, close to in situ concentrations. Mixotrophy may be the rule rather the exception in these experimental systems (Moore, 2013; Evans et al., 2015).

4.3 Phytoplankton-bacteria coupling and metabolic balance

Torréton et al. (2010) report mean Chl concentration around 0.3 $\mu g L^{-1}$ over a seasonal cycle performed at an oligotrophic station in the New Caledonia lagoon. These concentrations are close to our reference conditions outside the mesocosms (lagoon waters), where means of Chl values were 0.21 and 0.30 $\mu g L^{-1}$ during P1 ad P2 phases. Under these oligotrophic conditions, the seasonal variability of BP and PP in the Nouméa lagoon is much lower than in temperate waters, only about 3-fold with an average BP/PP ratio of 0.21, and some rare peaks reaching 0.6 (Torréton et al., 2010). This is in ac-

BGD
12, 19861–19900, 2015

cordance with the range of BP/PP ratios encountered in the lagoon waters during our study, with average values ranging 0.33 to 0.39 during phases P1 and P2, respectively. On the opposite, inside the mesocosms, average BP/PP ratios were generally higher than in the lagoon waters whatever the phase or the mesocosm considered. A negative trend of BP/PP with increasing PP was obtained, suggesting that a larger fraction of PP is channelled through the microbial food web when PP decreases, as observed in the oligotrophic Mediterranean Sea (Conan et al., 1999). This is also the trend when considering a large oceanic data set examined by Fouilland and Mostajir (2010). Indeed in their study, regression of log BP as a function of (log PP) resulted in a slope of 0.57, inferring that BP increases less rapidly than PP when PP increases. Contrarily to the weak (during P2) or absence of (during P1) correlation between BP and N_2 fixation rates described above, strong relationships between BP and Chl, and between BP and PP were obtained during both phases (Fig. 5). This suggests that N_2 fixation stimulated autotrophic communities during the VAHINE experiment, which may in turn have produced organic matter for heterotrophic prokaryotes. BP and PP are determined routinely, but to estimate the flux of PP channelled through heterotrophic bacteria, or to infer metabolic balance between autotrophy and heterotrophy, bacterial carbon demand (BCD) and gross primary production (GPP) must be also estimated. Such carbon fluxes are not directly estimated but are derived from PP and BP using additional measurements of bacterial growth efficiency (or bacterial respiration) and phytoplankton extracellular release of DOC. These parameters are less frequently acquired due to time-consuming and difficult technologies (del Giorgio and Cole, 1998; Nagata, 2000), which led to controversy on the metabolic balance in oligotrophic environments (Cole et al., 1988; Ducklow et al., 2002; Van Wambeke et al., 2008b; Fouilland and Mostajir, 2010; Moran and Alonzo-Saez, 2010). BCD is derived from BP by the use of bacterial growth efficiency (BGE) or respiration rates which are not often measured concomitantly with PP and BP, and in many oligotrophic environments BCD/PP is higher than 1, or respiration exceeds PP (del Giorgio et al., 1997). To explain this, different arguments are generally proposed. First, other DOM sources than those deriving from

BGD
12, 19861–19900, 2015

phytoplankton (allochthonous sources) are used to sustain BCD. In shallow lagoons, DOM released from benthos has been proposed as supplementary source of DOM for heterotrophic bacterioplankton (Torréton et al., 2002). Second, phasing between BP and PP peaks during seasonal blooms and occasional presence of PP bursts (see for example Steinberg et al., 2001) are not always detected due to inappropriate sampling frequency for BP and PP measurements. Daily and parallel measurements of both BP and PP in the mesoscosms avoided such problems in this study.

We used the advantage of a day to day sampling in an enclosed system to compute a carbon budget that will allow to estimate the fate of phytoplankton-derived organic carbon and the metabolic balance. This carbon budget was calculated using time-integrated data, and thus considered the whole data set. First, each time point was averaged for the three sampling depths, and then time integration was calculated separately for each mesocosm assuming a linear trend between 2 successive days. A mesocosm average was calculated based on the time-integrated data obtained in each of the three mesocosms, with error bars representing the standard deviation (sd) among the three mesocosms (Fig. 7a). Gross primary production (GPP) is derived from PP assuming GPP = PP × 1.72 (Moutin et al., 1999) and represents the whole photosynthetic source of organic matter, including both particulate and extracellular release forms. The cumulated GPP at day 23 was 38 ± 11 µM C (Fig. 7b). Carbon exported by sedimentation into the traps (Cexp) was corrected in µM C units based on a mean, constant water volume inside M1, M2, and M3 (see Berthelot et al., 2015 for details) and its cumulated value reached 6.4 ± 2.1 µM C on day 23. For POC and DOC, for which data were more irregular and showed outliers, we decided to calculate net variations of POC and DOC after a linear fit of the discrete data set between days 5 and 23 in each mesocosm (Table 4). POC increased linearly in M1 and M3 (0.12 and 0.48 µmol C L^{-1} d^{-1}, $r = 0.32$, $p < 0.03$ and $r = 0.70$, $p < 0.001$, respectively) and showed no trend in M2. A significant increase of DOC was only observed in M2 (Table 4). Due to the high sd resulting from variability in net variation of POC and DOC vs. time between the three mesocosms, the average accumulation of DOC and POC estimated for the car-

BGD
12, 19861–19900, 2015

bon budget was negligible (Fig. 7a), and the most important measured fate of GPP was Cexp, representing 17 % of GPP (Fig. 7b). GPP – (net DOC + net POC + Cexp) can be considered as community respiration (CR). CR was calculated and reached 27 ± 11 µM cumulated from day 5 to 23. However, it should be noted that CR was not directly measured, but obtained by difference, and that a biofilm developed at the end on the mesocosm walls as pointed out by Knapp et al. (2015). Assuming negligible effect of this biofilm on the plankton C budget, the main fate of photosynthetically fixed organic carbon during the experiment (deduced from carbon budget) was respiration. The different responses between the triplicate mesocosms led to a great propagation of errors and thus on the variability on CR/GPP ratio (70 ± 36 %). CR being lower than GPP, the biological system inside mesocosms was net autotrophic, with an upper error limit close to metabolic balance between autotrophy and heterotrophy.

In order to calculate the fraction of GPP that channeled, directly or indirectly, through the microbial food web, the bacterial carbon demand (BCD) must be estimated through additional estimates of bacterial respiration (BR) or bacterial growth efficiency (BGE). In an oligotrophic site inside the Nouméa lagoon, BGE was estimated at 10 % using incubated samples where oxygen changes were followed with time in the dark (Briand et al., 2004). However, as suggested by Aranguren-Gassis et al. (2012), using consistently low BGE derived from size fractionation experiments and long-duration incubations leads to probable BGE underestimation. In the lagoon, the use of a 10 % BGE would lead to BCD values higher than GPP (Rochelle-Newall et al., 2008). If we assume such low BGE in the mesocosms (10 %), cumulated BR from day 5 to 23 would rise to 93 ± 6 µM C, which is not realistic compared to CR estimated from the carbon budget. A more appropriate BGE of 27 to 43 % could be calculated, based on minimum and maximum ranges admitted for BR/CR ratio (from 100 to 50 %, Lemée et al., 2002). Such values are more reliable than BR estimates based on Electron Transport System measurements (Aranguren-Gassis et al., 2012) and are in agreement with the beneficial effect of photo-heterotrophy. Indeed, the BGE of a proteorhodopsin-containing strain (*Erythrobacter* sp.) was shown to increase during light periods in a continu-

BGD
12, 19861–19900, 2015

ous culture (Hauruseau et al., 2012). In a companion metatranscriptomic study performed in M1, accumulation of proteorhodopsin transcripts was recurrently detected among varying groups of bacteria notably SAR11 and SAR86 (Pfreundt et al., 2015a). These groups, belonging to the alpha- and gammaproteobacteria, respectively, also played key roles in the microbial comunity as observed through 16S sequencing (Pfreundt et al., 2015b). Heterotrophic bacteria are limited by N but also by energy in the South Pacific (Van Wambeke et al., 2008a); this could give an advantage to photoheterotrophic prokaryotes for growth and their success in this area.

Assuming BGE values ranging from 27 to 43 %, the BCD/GPP ratio would range from 63 to 99 %. A large part of the GPP is thus channelled through the microbial food web pathway within 20 days. To examine potential links between phytoplankton release and BP, we estimated a extracellular release of 35 %, as determined previously inside the Nouméa lagoon (Rochelle-Newall et al., 2008). Such values are in agreement with higher percent extracellular release that are generally obtained in nutrient limited environments (Nagata, 2000). According to Rochelle-Newall et al. (2008), contemporaneous DOC excreted by phytoplankton was sufficient to meet BCD only in the coastal part of the lagoon, but not in the offshore oligotrophic part of the lagoon where the VAHINE experiment was performed, but these authors used a 10 % BGE. In the mesocosms, still based on a extracellular release representing 35 % of GPP, DOC release was estimated at 13 µM C produced between 5–23 days. This is not sufficient to satisfy BCD cumulated for the same period (calculated as 24–38 µM C) although we used BGE varying from 27 to 43 % as discussed above. Thus, heterotrophic bacteria in the mesocosms used additional, not contemporaneous, sources of organic matter derived from phytoplankton after transformation through the food web like enzymatic hydrolysis of detritus, viral lysis, and/or sloppy feeding.

BGD
12, 19861–19900, 2015

5 Conclusions

This study confirms that in the Nouméa lagoon, N_2 fixation is a relevant process to fuel the microbial food web and to sustain a biological system which is net autotrophic or close to metabolic balance. The relatively high BGE computed from the carbon budget (27–43 %) could be related to light-harvesting systems developed by abundant bacterial heterotrophs. The success of *Synechococcus* over *Prochlorococcus* descibed in companion papers (Leblanc et al., 2015; Pfreundt et al., 2015b) might be attributed to their ability to assimilate leucine, and possibly other amino acids. Moreover, as indicated by the high expression of the sulfolipid biosynthesis gene *sqdB* (Pfreundt et al., 2015a), these cyanobacteria are able to reduce their cellular P demand through sulfolipid synthesis. The relative importance of mixotrophy in these oligotrophic system implies that it is important to (i) find alternative techniques to dark incubations to estimate bacterioplankton respiration and (ii) to detect organisms responsible for the assimilation of a wide variety of organic molecules by cell sorting. From the carbon budget, a BCD to GPP ratio was estimated to range between 63 and 100 %, and thus a large part of the primary production is channelled through the microbial food web. Bacterial production was strongly coupled with Chl biomass and/or PP, rather than with N_2 fixation rates, suggesting that indirect routes through lysis, grazing and mortality of phytoplankton were substantial for providing labile organic matter for heterotrophic bacteria.

Author contributions. S. Bonnet was the chief scientist responsible of the VAHINE program, she designed and executed the experiment in mesocosms. F. Van Wambeke sampled for and analyzed BP and APA, T. Moutin sampled for and analyzed TDIP and PP, A. Barani performed the cell sorting, wrote the corresponding M&M section and made Fig. 2, H. Berthelot contributed to the analyses of bacterial abundances by flow cytometry, M. Rodier sampled for and analyzed data, F. Van Wambeke and U. Pfreundt equally wrote the manuscript and made the other figures. All the authors reviewed the manuscript.

Acknowledgements. Funding for this research was provided by the Agence Nationale de la Recherche (ANR starting grant VAHINE ANR-13-JS06-0002), INSU-LEFE-CYBER program,

BGD
12, 19861–19900, 2015

GOPS, IRD and M.I.O. The participation of UP and WRH was supported by the German-Israeli Research Foundation (GIF), project number 1133–13.8/2011 and the MiSeq-based microbial community analysis by the EU project MaCuMBA (Marine Microorganisms: Cultivation Methods for Improving their Biotechnological Applications; grant agreement no: 311 975) to WRH. The authors thank the captain and crew of the R/V *Alis*. We acknowledge the SEOH divers service from the IRD research center of Nouméa (E. Folcher, B. Bourgeois and A. Renaud) and from the Observatoire Océanologique de Villefranche-sur-mer (OOV, J.M. Grisoni) as well as the technical service of the IRD research center of Noumé a for their helpful technical support. C. Guieu, F. Louis and J.M. Grisoni from OOV are warmly thanked for the mesocosms design and their useful advice for deployment. We are grateful to the Regional Flow Cytometry Platform for Microbiology (PRECYM) of the Mediterranean Institute of Oceanography (MIO) for the flow cytometry analyses. We acknowledge Anne Desnues for help in sampling, Karine Leblanc, Bruno Charrière and Jules Héliou for analyzing TOC, POC and Chl data.

References

Aranguren-Gassis, M., Teira, E., Serret, P., Martínez-García, M., and Fernández, E.: Potential overestimation of bacterial respiration rates in oligotrophic plankton communities, Mar. Ecol.-Prog. Ser., 453, 1–10, 2012.

Béjà, O. and Suzuki, M.: Photoheterotrophic marine prokaryotes, in: Microbial Ecology of the Oceans, 2nd edn., edited by: Kirchman, D., John Wiley & Sons, Inc, 131–157, 2008.

Berman-Frank, I., Spungin, D., Rahav, E., Van Wambeke, F., Berthelot, H., Turk-Kubo, K., Bonnet, S., and Moutin, T.: Dynamics of Transparent Exopolymer Particles (TEP) during a mesocosm experiment in the New Caledonia lagoon, Biogeosciences Discuss., this issue, 2015.

Berthelot, H., Moutin, T., L'Helguen, S., Leblanc, K., Hélias, S., Grosso, O., Leblond, N., Charrière, B., and Bonnet, S.: Dinitrogen fixation and dissolved organic nitrogen fueled primary production and particulate export during the VAHINE mesocosm experiment (New Caledonia lagoon), Biogeosciences, 12, 4099–4112, doi:10.5194/bg-12-4099-2015, 2015.

Biegala, I. and Raimbault, P.: High abundance of diazotrophic pico-cyanobacteria (< 3 µm) in a south-west Pacific coral lagoon, Aquat. Microb. Ecol., 51, 45–53, 2008.

Bonnet, S., Guieu, C., Bruyant, F., Prášil, O., Van Wambeke, F., Raimbault, P., Moutin, T., Grob, C., Gorbunov, M. Y., Zehr, J. P., Masquelier, S. M., Garczarek, L., and Claustre, H.:

BGD
12, 19861–19900, 2015

Nutrient limitation of primary productivity in the Southeast Pacific (BIOSOPE cruise), Biogeosciences, 5, 215–225, doi:10.5194/bg-5-215-2008, 2008.
Bonnet, S., Berthelot, H., Turk-Kubo, K., Fawcett, S., Rahav, E., Berman-Frank, I., and l'Helguen, S.: Dynamics of N2 fixation and fate of diazotroph-derived nitrogen in a low nutrient low chlorophyll ecosystem: results from the VAHINE mesocosm experiment (New Caledonia) S. Bonnet, H. Berthelot, K. Turk-Kubo, S. Fawcett, E. Rahav, S. l'Helguen, and I. Berman-Frank Biogeosciences Discuss., 12, 19579–19626, 2015a, http://www.biogeosciences-discuss.net/12/19579/2015/.
Bonnet, S., Moutin, T., Rodier, M., Grisoni, J. M., Louis, F., Folcher, E., Bourgeois, B., Boré J. M. , and Renaud, A.: Introduction to the VAHINE project: VAriability of vertical and tropHIc transfer of fixed N_2 in the south wEst Pacific, Biogeosciences Discuss., this issue, 2015b.
Bonnet, S., Rodier, M., Turk-Kubo, K., Germineaud, C., Menkes, C., Ganachaud, A., Cravatte, S., Raimbault, P., Campbell, E., Quéroué, F., Sarthou, G., Desnues, A., Maes, C., and Eldin, G.: Contrasted geographical distribution of N_2 fixation rates and nifH phylotypes in the Coral and Solomon Seas (South-Western Pacific) during austral winter conditions, Global Biogeochem. Cy., 29, in press, doi:10.1002/2015GB005117, 2015c.
Briand, E., Pringault, O., Jacquet, S., and Torréton, J.-P.: The use of oxygen microprobes to measure bacterial respiration for determining bacterioplankton efficiency, Limnol. Oceanogr.-Meth., 2, 406–416, 2004.
Cole, J. J., Findlay, S., and Pace, M. L.: Bacterial production in fresh and saltwater ecosystems: a cross – system overview, Mar. Ecol.-Prog. Ser., 43, 1–10, 1988.
Conan, P., Turley, C., Stutt, E., Pujo-Pay, M., and Van Wambeke, F.: Relationship between phytoplankton efficiency and the proportion of bacterial production to primary production in the Mediterranean Sea, Aquat. Microb. Ecol., 17, 131–144, 1999.
del Giorgio, P. A. and Cole, J. J.: Bacterial growth efficiency in natural aquatic systems, Annu. Rev. Ecol. Syst., 29, 503–541, 1998.
del Giorgio, P., Cole, J. J., and Cimbleris, A.: Respiration rates in bacteria exceeds phytoplankton production in unproductive aquatic systems, Nature, 385, 148–151, 1997.
Ducklow, H. W., Kirchman, D. L., and Anderson, T. R.: The magnitude of spring bacterial production in the North Atlantic Ocean, Limnol. Oceanogr., 47, 1684–1693, 2002.
Evans, C., Gómez-Pereira, P. R., Martin, A. P., Scanlan, D., and Zubkov, M. V.: Photoheterotrophy of bacterioplankton is ubiquitous in the surface oligotrophic ocean, Prog. Oceanogr., 135, 139–145, 2015.

BGD
12, 19861–19900, 2015

Fouilland, E. and Mostajir, B.: Revisited phytoplanktonic carbon dependencyof heterotrophic bacteria infreshwaters, transitional, coastal and oceanic waters, FEMS Microbiol. Ecol., 73, 419–429, 2010.
Fukuda, R., Ogawa, H., Nagata, T., and Koike, I.: Direct determination of carbon and nitrogen contents of natural bacterial assemblages in marine environments, Appl. Environ. Microb., 64, 3352–3358, 1998.
Garcia, N., Raimbault, P., and Sandroni, V.: Seasonal nitrogen fixation and primary production in the Southwest Pacific: nanoplankton diazotrophy and transfer of nitrogen to picoplankton organisms, Mar. Ecol.-Prog. Ser., 343, 25–33, 2007.
Gimenez, A., Baklouti, M., Bonnet, S., Moutin, T.: Impact of a phosphate enrichment on biogeochemical fluxes and fate of diazotroph derived nitrogen: modelling of the VAHINE mesocosms experiment, Biogeosciences Discuss., this issue, 2015.
Guieu, C., Dulac, F., Desboeufs, K., Wagener, T., Pulido-Villena, E., Grisoni, J.-M., Louis, F., Ridame, C., Blain, S., Brunet, C., Bon Nguyen, E., Tran, S., Labiadh, M., and Dominici, J.-M.: Large clean mesocosms and simulated dust deposition: a new methodology to investigate responses of marine oligotrophic ecosystems to atmospheric inputs, Biogeosciences, 7, 2765–2784, doi:10.5194/bg-7-2765-2010, 2010.
Halm, H., Lam, P., Ferdelman, T. G., Lavik, G., Dittmar, T., LaRoche, J., D'Hondt, S., and Kuypers, M.: Heterotrophic organisms dominate nitrogen fixation in the South Pacific Gyre, ISME J., 6, 1238–1249, 2012.
Hauruseau, D. and Koblížek, M.: Influence of light on carbon utilization in aerobic anoxygenic phototrophs, Appl. Environ. Microb., 78, 7414–7419, 2012.
Hoppe, H. G.: Significance of exoenzymatic activities in the ecology of brackish water: measurement by means of methylumbelliferyl-substrates, Mar. Ecol.-Prog. Ser., 11, 299–308, 1983.
Kirchman, D. L.: Leucine incorporation as a measure of biomass production by heterotrophic bacteria, in: Handbook of Methods in Aquatic Microbial Ecology, edited by: Kemp, P. F., Sherr, B. F., Sherr, E. B., and Cole, J. J., Lewis, Boca Raton, 509–612, 1993.
Knapp, A. N., Fawcett, S. E., Martinez-Garcia, A., Haug, G., Leblond, N., Moutin, T., and Bonnet, S.: Nitrogen isotopic evidence for a shift from nitrate- to diazotroph-fueled export production in VAHINE mesocosm experiments, Biogeosciences Discuss., this issue, 2015.

BGD
12, 19861–19900, 2015

Leblanc, K., Cornet, V., Caffin, M., Rodier, M., Desnues, A., Berthelot, H., Heliou, J., and Bonnet, S.: Phytoplankton community structure in the VAHINE MESOCOSM experiment, Biogeosciences Discuss., this issue, 2015.
Lemée, R., Rochelle-Newall, E., Van Wambeke, F., Pizay, M.-D., Rinaldi, P., and Gattuso, J.-P.: Seasonal variation of bacterial production, respiration and growth efficiency in the open NW Mediterranean Sea, Aquat. Microb. Ecol., 29, 227–237, 2002.
Marie, D., Partenski, F., Jaquet, S., and Vaulot, D.: Enumeration and cell cycle analysis of natural population of marine picoplankton by flow cytometry using the nucelic acid stain SYBR green I, Appl. Environ. Microb., 63, 186–193, 1997.
Mary, I., Garczarek, L., Tarran, G. A., Kolowrat, C., Terry, M. J., Scanlan, D. J., Burkill, P. H., and Zubkov, M. V.: Diel rhythmicity in amino acid uptake by Prochlorococcus, Environ. Microbiol., 10, 2124–2131, 2008a.
Mary, I., Tarran, G. A., Warwick, P. E., Terry, M. J., Scanlan, D. J., Burkill, P. H., and Zubkov, M. V.: Light enhanced amino acid uptake by dominant bacterioplankton groups in surface waters of the Atlantic Ocean, FEMS Microbiol. Ecol., 63, 36–45, 2008b.
Moisander, P. H., Beinart, R. A., Hewson, I., White, A. E., Johnson, K. S., Carlson, C. A., Montoya, J. P., and Zehr, J. P.: Unicellular cyanobacterial distributions broaden the oceanic N_2 fixation domain, Science, 327, 1512–1514, 2010.
Moore, L. R.: More mixotrophy in the marine microbial mix, P. Natl. Acad. Sci. USA, 110, 8323–8324, 2013.
Moran, X. A. and Alonso-Saez, L.: Independence of bacteria on phytoplankton?, Insufficient support for Fouilland & Mostajir's (2010) suggested new concept, FEMS Microbiol. Ecol., 78, 203–205, 2011.
Moutin, T., Raimbault, P., and Poggiale, J. C.: Production primaire dans les eaux de surface de la Méditerranée occidentale: calcul de la production journalière, CR Acad. Sci. III-Vie, 322, 651–659, 1999.
Moutin, T., Van Den Broock, N., Becker, B., Dupouy, C., Rimmelin, P., and Le Bouteiller, A.: Phosphate availability controls *Trichodesmium* spp. biomass in the SW Pacific Ocean, Mar. Ecol.-Prog. Ser., 297, 15–21, doi:10.3354/meps297015, 2005.
Moutin, T., Karl, D. M., Duhamel, S., Rimmelin, P., Raimbault, P., Van Mooy, B. A. S., and Claustre, H.: Phosphate availability and the ultimate control of new nitrogen input by nitrogen fixation in the tropical Pacific Ocean, Biogeosciences, 5, 95–109, doi:10.5194/bg-5-95-2008, 2008.

BGD
12, 19861–19900, 2015

Nagata, T.: Production mechanisms of dissolved organic matter, in: Microbial Ecology of the Oceans, edited by: Kirchman, D., Wiley Liss, 121–152, 2000.
Neveux, J., Lefebvre, J.-P., Le Gendre, R., Dupouy, C., Gallois, F., Courties, C., Gérard, P., Fernandez, J.-M., and Ouillon, S.: Phytoplankton dynamics in the southern New Caledonian lagoon during a southeast trade winds event, J. Marine Syst., 82, 230–244, 2010.
Pfreundt, U., Spungin, D., Bonnet, S., Berman-Frank, I., and Hess, W. R.: Global analysis of gene expression dynamics within the marine microbial community during the VAHINE mesocosm experiment in the South West Pacific, Biogeoscience Discuss., this issue, 2015a.
Pfreundt, U. Van Wambeke, F., Bonnet, S., and Hess, W. R.: Comparative analysis of the prokaryotic diversity during the VAHINE experiment, an experimental ecosystem challenge in the New Caledonia lagoon, Biogeoscience Discuss., this issue, 2015b.
Richardson, T. B. and Porter, C. D.: Inactivation of murine leukaemia virus by exposure to visible light, Virology, 341, 321–329, 2005.
Rochelle-Newall, E. J., Torréton, J.-P., Mari, X., and Pringault, O.: Phytoplankton–bacterioplankton coupling in a subtropical South Pacific coral reef lagoon, Aquat. Microb. Ecol., 50, 221–229, 2008.
Sieracki, M. E., Haugen, E. M., and Cucci, T. L.: Overestimation of heterotrophic bacteria in the Sargasso Sea: direct evidence by flow and imaging cytometry, Deep-Sea Res. II, 42, 1399–1409, 1995.
Smith, D. C. and Azam, F.: A simple, economical method for measuring bacterial protein synthesis rates in sea water using 3H-Leucine, Mar. Microb. Food Webs, 6, 107–114, 1992.
Steinberg, D. K., Carlson, C. A., Bates, N. R., Johnson, R. J., Michaels, A. F., and Knap, A. H.: Overview of the US JGOFS Bermuda Atlantic Time-series Study (BATS): a decade-scale look at ocean biology and biogeochemistry, Deep-Sea Res. II, 48, 1405–1447, 2001.
Talarmin, A., Van Wambeke, F., Catala, P., Courties, C., and Lebaron, P.: Flow cytometric assessment of specific leucine incorporation in the open Mediterranean, Biogeosciences, 8, 253–265, doi:10.5194/bg-8-253-2011, 2011.
Torréton, J. P., Pages, J., and Talbot, V.: Relationships between bacterioplankton and phytoplankton biomass, production and turnover rate in Tuamotu atoll lagoons, Aquat. Microb. Ecol., 28, 267–277, 2002.
Torréton, J.-P., Rochelle Newall, E., Pringault, O., Jacquet, S., Faure, V., and Brand, E.: Variability of primary and bacterial production in a coral reef lagoon (New Caledonia), Mar. Pollut. Bull., 61, 335–348, 2010.

BGD
12, 19861–19900, 2015

Turk-Kubo, K. A., Frank, I. E., Hogan, M. E., Desnues, A., Bonnet, S., and Zehr, J. P.: Diazotroph community succession during the VAHINE mesocosms experiment (New Caledonia Lagoon), Biogeosciences Discuss., 12, 9043–9079, doi:10.5194/bgd-12-9043-2015, 2015.

Van Wambeke, F., Bonnet, S., Moutin, T., Raimbault, P., Alarcón, G., and Guieu, C.: Factors limiting heterotrophic bacterial production in the southern Pacific Ocean, Biogeosciences, 5, 833–845, doi:10.5194/bg-5-833-2008, 2008a.

Van Wambeke, F., Obernosterer, I., Moutin, T., Duhamel, S., Ulloa, O., and Claustre, H.: Heterotrophic bacterial production in the eastern South Pacific: longitudinal trends and coupling with primary production, Biogeosciences, 5, 157–169, doi:10.5194/bg-5-157-2008, 2008b.

Zubkov, M. V., Tarran, G. A., and Fuchs, B. M.: Depth related amino acid uptake by Prochlorococcus cyanobacteria in the southern Atlantic tropical gyre, FEMS Microbiol. Ecol., 50, 153–161, 2004.

BGD
12, 19861–19900, 2015

Table 1. Averages ± SD of some parameters during phases P1 (from day 5 to day 14) and P2 (from day 15 to day 23) in the three mesocosms M1, M2, M3 and in the lagoon waters (out). HBA: heterotrophic prokaryotic abundances, BP: heterotrophic prokaryotic production, AOA: alkaline phosphatase activity, TDIP: turnover time of DIP. N_2 fixation contribution to BP (N_2fix/BP ratio, in %) is based on a C/N of 6.8 for heterotrophic bacteria. Mann–Whiney tests were performed to test significant differences between P1 and P2: [a] $p < 0.05$; [b] $0.01 < p < 0.05$; [c] $p < 0.001$.

	M1 P1	M1 P2	out P1	out P2
Chl ($\mu g\,L^{-1}$)	0.19 ± 0.05^{c}	0.42 ± 0.14	0.21 ± 0.03^{c}	0.30 ± 0.07
% pheopigments	24 ± 3^{c}	28 ± 5	23 ± 6	26 ± 3
HBA ($\times 10^5$ cells mL^{-1})	3.9 ± 1.9	4.5 ± 1.7	na	na
PP ($\mu mol\,C\,L^{-1}\,d^{-1}$)	0.71 ± 0.27^{c}	1.09 ± 0.22	0.85 ± 0.17^{c}	1.36 ± 0.37
BP ($ng\,C\,L^{-1}\,h^{-1}$)	157 ± 49^{c}	348 ± 42	135 ± 24^{c}	256 ± 60
DOC µM C	59 ± 3	60 ± 2	60 ± 3	60 ± 2
POC µM C	8 ± 3^{a}	9 ± 1	6.6 ± 1.1^{b}	7.6 ± 1.3
APA (nmole MUF-P hydr $L^{-1}\,h^{-1}$)	1.5 ± 0.9^{c}	8.0 ± 5.4	3.0 ± 2.3^{b}	5.0 ± 3.1
TDIP (days)	16 ± 15^{c}	0.5 ± 0.3	2.0 ± 0.9^{c}	0.9 ± 0.4
BP/PP ratio	0.48 ± 0.18^{c}	0.65 ± 0.20	0.33 ± 0.11^{a}	0.39 ± 0.10
N_2 fix / BP ratio (%)	21 ± 11^{a}	29 ± 16	22 ± 13^{a}	15 ± 8

	M2 P1	M2 P2	M3 P1	M3 P2
Chl ($\mu g\,L^{-1}$)	0.22 ± 0.03^{c}	0.49 ± 0.18	0.20 ± 0.04^{c}	0.71 ± 0.30
% pheopigments	23 ± 2^{c}	28 ± 6	23 2	26 ± 15
HBA ($\times 10^5$ cells mL^{-1})	2.2 ± 2.2	4.9 ± 1.8	4.1 ± 0.7^{a}	5.0 ± 1.4
PP ($\mu mol\,C\,L^{-1}\,d^{-1}$)	0.75 ± 0.15^{c}	1.47 ± 0.35	0.73 ± 0.15^{c}	2.45 ± 0.76
BP ($ng\,C\,L^{-1}\,h^{-1}$)	227 ± 114^{c}	338 ± 116	168 ± 52^{c}	422 ± 132
DOC µM C	58 ± 3^{b}	61 ± 1	61 ± 3	60 ± 2
POC µM C	10 ± 3	9 ± 1	9 ± 2^{c}	13 ± 3
APA (nmole MUF-P hydr $L^{-1}\,h^{-1}$)	1.0 ± 0.8^{c}	7.6 ± 7.6	0.6 ± 0.5^{c}	3.18 ± 2.61
TDIP (days)	27 ± 19^{c}	1.8 ± 2.0	25 ± 12^{c}	3.0 ± 3.1
BP/PP ratio	0.65 ± 0.41	0.47 ± 0.16	0.50 ± 0.24^{a}	0.35 ± 0.08
N_2 fix / BP ratio (%)	17 ± 16^{c}	30 ± 18	25 ± 15	22 ± 11

BGD
12, 19861–19900, 2015

Table 2. Log–Log relationships between BP/PP ratio and PP (expressed in $mg\,C\,m^{-3}\,d^{-1}$). In mesocosms, phase P1 and P2 are separated for the regressions. r: Pearson correlation coefficient, p: probability.

	equation	r	probability
phase P1	$\log BP/PP = -0.87 \log PP + 0.49$	0.59	< 0.001
phase P2	$\log BP/PP = -0.53 \log PP + 0.33$	0.6	< 0.001
lagoon waters	$\log BP/PP = -0.24 \log PP - 0.19$	0.28	< 0.01

BGD
12, 19861–19900, 2015

Table 3. Specific leucine activities of main phytoplankton groups sorted. PRO: *Prochlorococcus*, LO-SYN (low orange fluorescence *Synechococcus*-like cells), HO-SYN (high orange fluorescence *Synechococcus*-like cells, PE (pico-eukaryotes) and bulk (total community leucine incorporation rates) corresponding to the same sample. When tests of reproducibility have been done, the corresponding data is indicated with its standard error. bdl: below detection limits.

	PRO	LO SYN	HO SYN	PE	bulk
		$\times 10^{-21}$ mole leu cell^{-1} h^{-1}			pmole leu L^{-1} h^{-1}
d15 M1	bdl	4.6 ± 1.9	3.5 ± 0.3	19 ± 5	97 ± 3
d19 M1	bdl	5.4	3.5	17	126 ± 3
d21 out	69 ± 28	30 ± 4	25 ± 4	79 ± 12	186 ± 6
d23 M1	22	131	42	108	242 ± 7

BGD
12, 19861–19900, 2015

Table 4. Linear regression fits on temporal trends of POC and DOC in M1, M2 and M3 from days 5 to 23. DOC has been sampled only at 6 m depth in the 3 mesocosms. df: degree of freedom, r: Pearson correlation coefficient, p: probability, ns: not significant. For POC trend, some outliers have been suppressed from the regressions.

	Range µM	Outliers µM	slope	df	r	p
POC M1	4.7–12.4	19.3	0.12	35	0.32	0.02
POC M2	7.1–11.6	15.0, 15.0, 17.3	−0.009	28	0.03	ns
POC M3	6.5–18.9	no	0.47	36	0.70	< 0.001
DOC M1	54–64	no	0.071	13	0.15	ns
DOC M2	53–62	no	0.25	13	0.48	0.04
DOC M3	54–66	no	−0.12	14	0.22	ns

BGD
12, 19861–19900, 2015

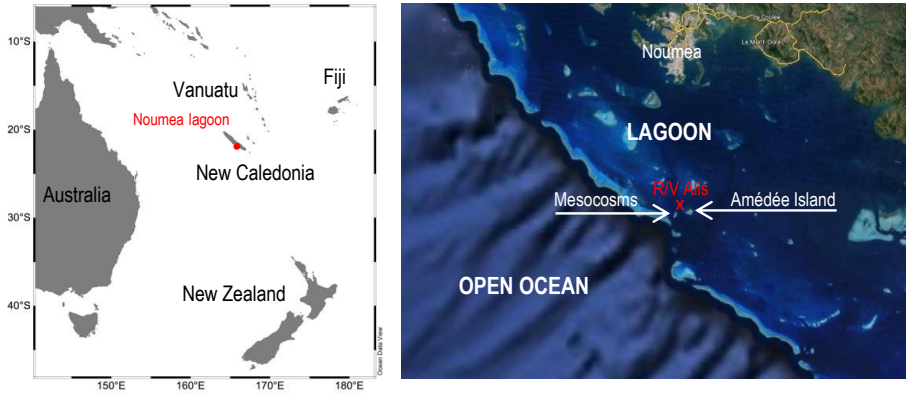

Figure 1. Position of mesocosms implemented in the southwest lagoon of New Caledonia.

BGD
12, 19861–19900, 2015

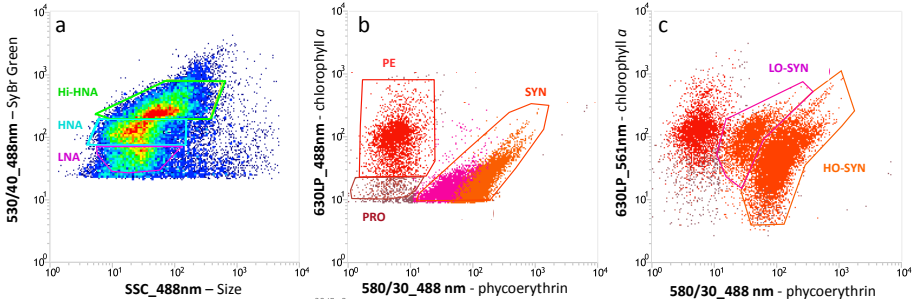

Figure 2. Example of flow cytometry cytogram dot plot of: **(a)** naturally non-fluorescent bacterioplankton groups discriminated by their DNA content (SYBR green-induced fluorescence in arbitrary units (a.u.) vs. cell size (side scatter), after 488 nm laser excitation); **(b)** phototrophic groups discriminated by their chlorophyll *a* content (related to the red fluorescence intensity (a.u.) vs. phycoerythrin related to the orange fluorescence intensity (a.u.) after 488 nm laser excitation); **(c)** low-orange (LO-SYN) and high-orange (HO-SYN) *Synechococcus*-like sub-groups separated by their chlorophyll *a* content (after 661 nm laser excitation) vs. their phycoerythrin content (after 488 nm laser excitation).

BGD
12, 19861–19900, 2015

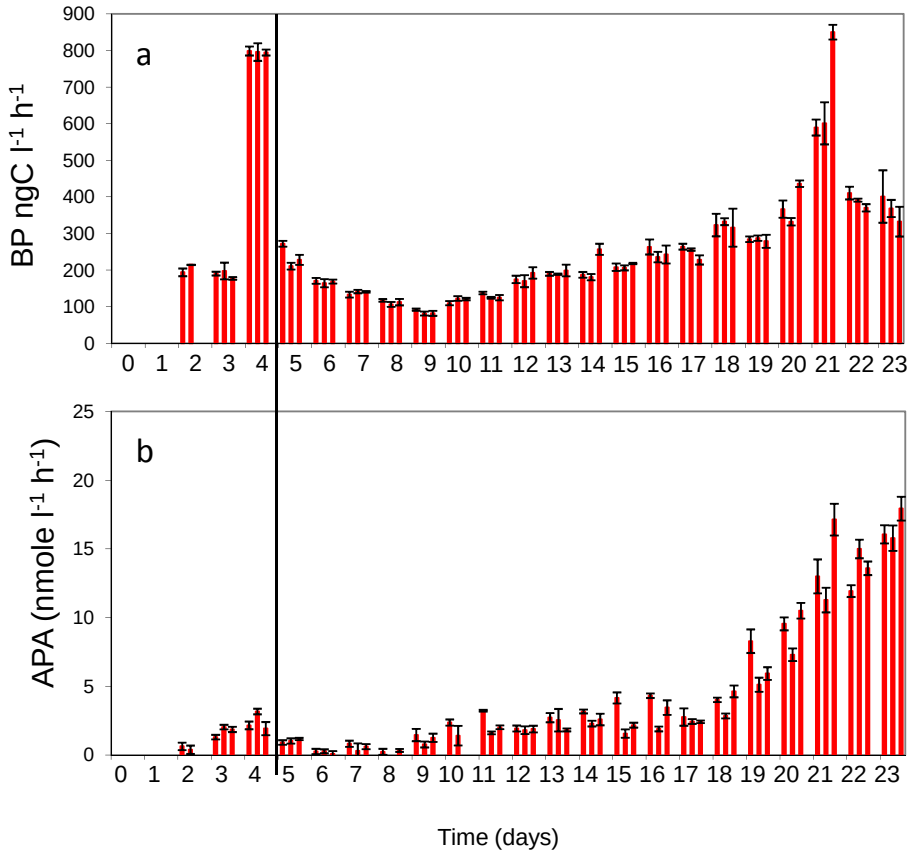

Figure 3. Evolution of: **(a)** bacterial production and **(b)** alkaline phosphatase in the mesocosm M1 at the three depths sampled. For each day 1, 6 and 12 m are presented from left to right. For the BP plot error bars are standard deviations within triplicate measurements. For phosphatase activity, error bars are the standard errors of the slope of the linear regression MUF production as a function of time. The vertical bar between day 4 and 5 indicates DIP fertilization.

BGD
12, 19861–19900, 2015

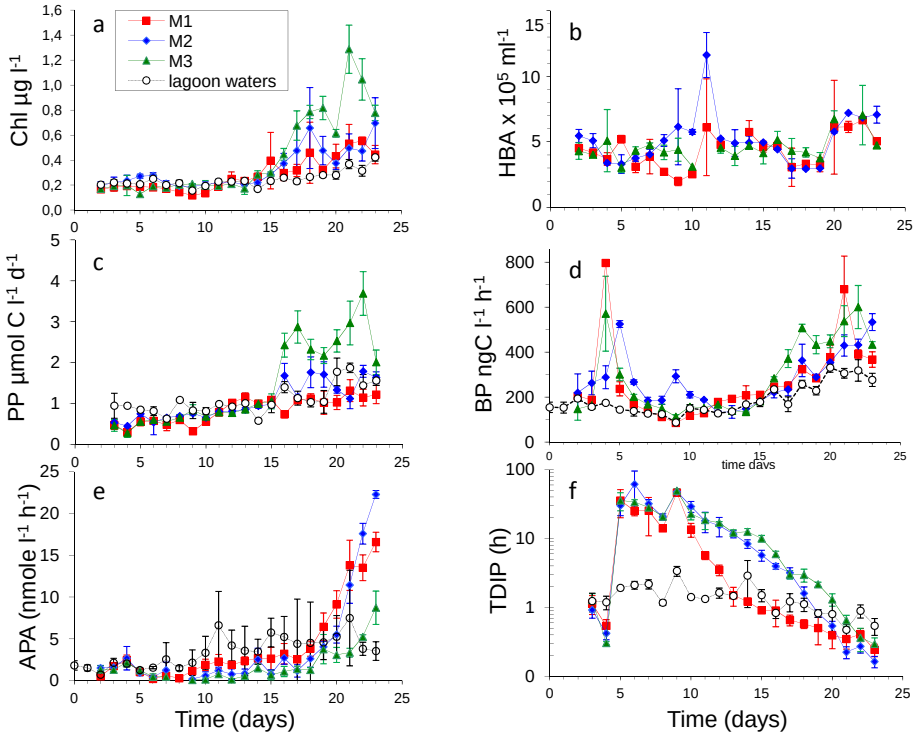

Figure 4. Evolution of: **(a)** chlorophyll *a* (Chl), **(b)** heterotrophic bacterial abundance (HBA), **(c)** primary production (PP), **(d)** heterotrophic bacterial production (BP), **(e)** alkaline phosphatase activity (APA) and **(f)** DIP turnover time (TDIP) in the three mesocosms M1, M2, M3 and in the lagoon waters (lagoon). Each point is the mean of the three depths sampled, error bars are standard deviations.

BGD
12, 19861–19900, 2015

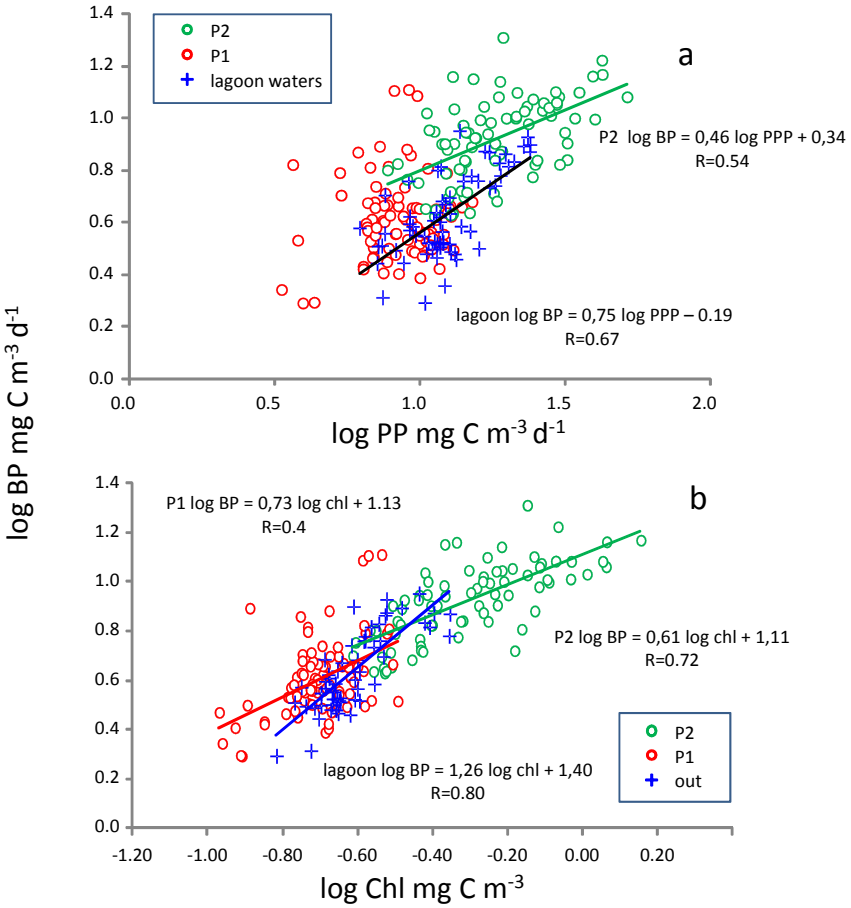

Figure 5. Log–log relationships between heterotrophic bacterial production (BP) and **(a)** primary production (PP) or **(b)** chlorophyll *a* (Chl).

BGD
12, 19861–19900, 2015

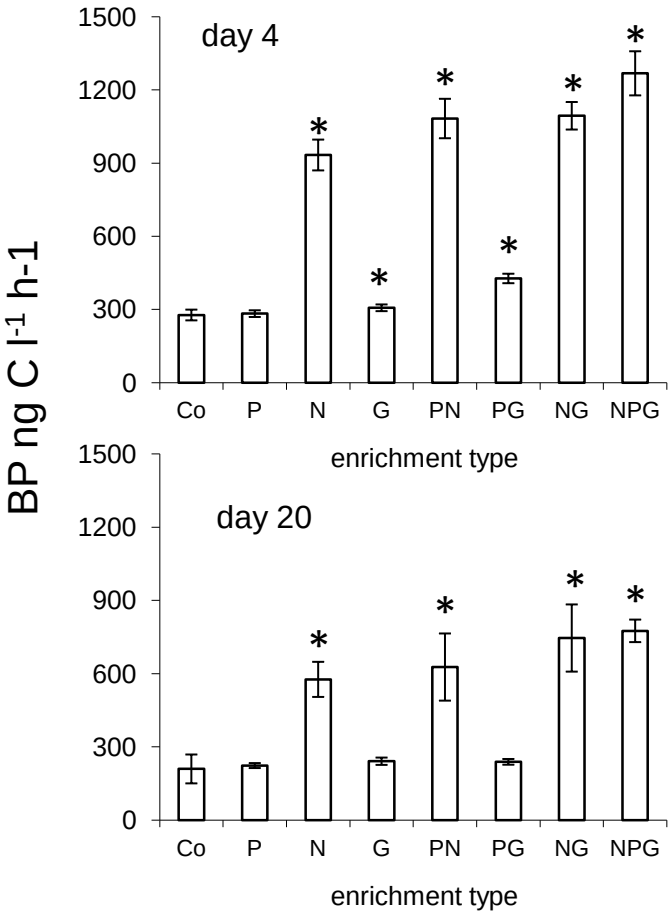

Figure 6. Response of heterotrophic bacterial production to the enrichment experiments conducted on days 4 and 20. Asterisks show significant responses in comparison to the unamended control (Co) after Mann Whitney test (*: $p < 0.05$).

BGD
12, 19861–19900, 2015

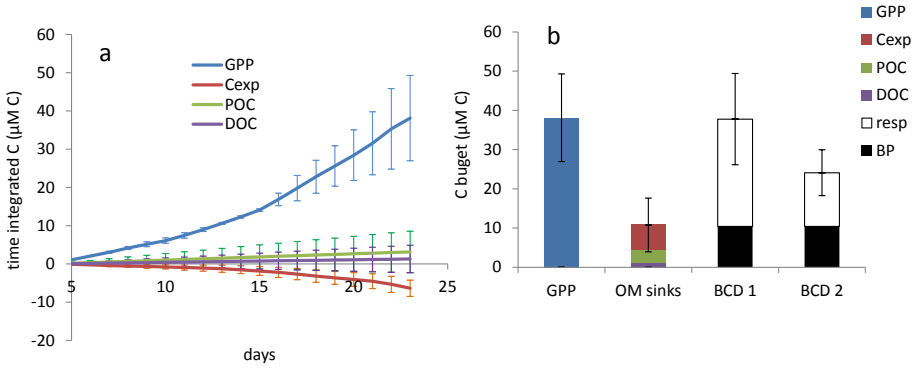

Figure 7. Carbon budget of the mesocosms with time (µM C). **(a)** Evolution of time-integrated gross primary production (GPP). Cexp: C export in sediment traps (Cexp), time-integrated net POC and net DOC are calculated assuming linear fits of these variables between days 5 and 23 (see Table 3). **(b)** Budget of time-integrated data on day 23. The difference GPP – (Cexp + net DOC + net POC) was assumed to be community respiration (resp). The range of heterotrophic bacterial carbon demand (BCD) was calculated based on two hypotheses: BR = 100 % CR (DCB1) or BR = 50 % CR (DCB2). Error bars are plotted from the sum of each category, using propagation of errors.

BGD
12, 19861–19900, 2015